Performance of First and Second-Order Sliding Mode Observers for Nonlinear Systems

A. Samir Herek[1], Steven Su[1], H. Trinh[2] , and Q. P. Ha[1]

[1] *Faculty of Engineering and Information Technology,*
University of Technology, Sydney
PO Box 123 Broadway NSW 2007 Australia

[2] *School of Engineering*
Deakin University,
Geelong 3217, Australia

Abstract

This paper presents a brief study on the design and performance comparison of conventional first-order and super-twisting second-order sliding mode observers for some nonlinear control systems. Estimation accuracy, fast response, chattering effect, peaking phenomenon and robustness are considered for nonlinear systems under observer-based output feedback control and state feedback control.

1. Introduction

The concept of an observer for a dynamic process was introduced in 1966 by Luenberger [1]. Years later many advanced observers have been presented. During that time, pioneering work in variable structure systems with sliding modes also emerged in the former Soviet Union [2]. Sliding mode techniques have been recognised as a robust control method, whereby a variable structure control is suitably chosen to drive and then constrain the system state to lie within a desired sliding surface. The sliding mode methodology has been applied to the observer design problem to retain the unique property in that it ensures the accurate convergence of the state estimates while sliding motion is induced for the estimation error dynamics [3].

Since the earliest work by Slotine *et al*. in the mid 1980s [4], sliding mode observers have been widely used due to their salient advantages such as robustness against uncertainties, finite-time convergence, and possibility of estimating unknown inputs, e.g. friction [3,5,6]. A conventional first-order sliding mode observer (SMO) requires the relative degree between the system inputs and outputs to be one and quite often involves chattering. To overcome these limitations while preserving SMO advantageous properties, higher sliding modes have been proposed for both control and observation (see, e.g., [7], [8]). The main difference between conventional and higher order sliding mode is that higher order derivatives of the sliding function are used in place of first-order derivatives. This is also required when the time rate of the control signal is used to achieve the control objective [9].

A new generation of observers based on the second-order sliding-mode algorithms has been recently developed [5]. These include the use of second-order SMOs for velocity estimation for uncertain, nonlinear mechanical systems [10], estimation of the absolute orientation of a five-link biped robot [11], estimation of road profile [12] and vehicle dynamic parameters of the road/vehicle interaction [13], or fault detection and isolation in permanent magnet synchronous motors [14]. Notably, higher-order SMOs based on twisting algorithms do not require the relative degree to be one and can totally remove chattering [5]. These merits can lead to exact differentiation of signals, which turns out to be very promising for health monitoring and fault diagnosis in many practical systems as the estimation of errors of the derivatives will be small if the magnitude of noise is small [5].

The use the super twisting algorithm, which is based on an exact and robust sliding mode differentiator of second order [7], facilitates the need for higher order derivatives in higher order SMOs. In [15], the algorithm is used in designing observers for hybrid systems to avoid chattering and time delays in a class of switched chaotic systems. For the challenging problem of simultaneous estimation of state and unknown input for nonlinear systems (see, e.g [16]), higher-order SMOs are also expected to be of great potential. This paper, motivated by a comparison study on advanced state observer design techniques [17], evaluates performance of first- and second-order SMOs and presents advantages of the super-twisting second-order sliding mode observers over the conventional SMOs. Simulation results are given for some nonlinear systems in state feedback and also output feedback.

2. Sliding Mode Observers

2.1 First order SMO:

Consider a *n-th* order continuous time system with state vector $x(t) \in R^n$, input $u(t) \in R^p$ and measurable output $y(t) \in R^m$:

$$\dot{x} = Ax + f(x,u) \quad (1a)$$
$$y = Cx, \quad (1b)$$

where (A,C) is an observable pair, $f(x,u)$ is a nonlinear vector function locally Lipschitz in x with a Lipchitz constant γ:

$$\|f(x_1,u) - f(x_2,u)\| \le \gamma \|x_1 - x_2\|, \ \forall (x_1,x_2), \forall u, \quad (2)$$

and γ >0 is a positive scalar.

The first-order sliding mode observer can be obtained as [18]:

$$\dot{\hat{x}} = A\hat{x} + f(\hat{x},u) + L\,(y - C\hat{x}) + S(\hat{x}, y), \quad (3)$$

where L is a constant gain matrix obtained by assigning the observer desired dynamics, i.e., stable eigenvalues $eig(A-LC)$,

$$S(\hat{x}, y) = \begin{cases} P^{-1}C^T sign(Ce_x) & , \quad \|Ce_x\| > \varepsilon \\ \dfrac{P^{-1}C^T \ \ Ce_x}{\varepsilon} & , \quad \|Ce_x\| \le \varepsilon \end{cases} \quad (4)$$

with $e_x = x - \hat{x}$, or $Ce_x = y - C\hat{x}$, ε >0 is the amplitude of a boundary layer, and P is a symmetric positive definite matrix solving for the following algebraic Riccati equation:

$$(A - LC)^T P + P(A - LC) + I + \gamma^2 PP = -Q, \quad (5)$$

for a given symmetric positive definite matrix $Q > 0$. It can be shown that the error system of observer (2) under the variable structure term (4) asymptotically converges to zero or remains bounded in the case of noisy measurements [18].

Remark 1: Given a Lipschitz constant γ >0, one can further relax (5) into an inequation in order to conveniently compute P by using a linear matrix inequality (LMI) formulation:

$$\begin{bmatrix} (A - LC)^T P + P(A - LC) + I & \gamma P \\ \gamma P & -I \end{bmatrix} > 0, \quad (6)$$

where γ =0 in the case of linear systems.

2. Second-order SMO:

For the design of a higher-order sliding mode observer, let us consider system (1) in a canonical form as follows:

$$\begin{aligned} \dot{x}_1 &= x_2 \\ \dot{x}_2 &= f(x_1,x_2,u) + \xi(x_1,x_2,u), \end{aligned} \quad (7)$$

where $[x_1^T(t)\ x_2^T(t)]^T \in R^{2n}$ is the system state, $u(t) \in R^n$ is the control, $y(t) = x_1(t)$ is the measurable output, and the system nonlinear function $f(x_1,x_2,u)$ is known and perturbed by uncertainty $\xi(x_1,x_2,u)$, where f and ξ are Lebesgue-measurable in any compact region of the state space (x_1,x_2). As physical states of a practical system are bounded, it is assumed the existence of a finite constant f^+ >0 such that for any $(x_1,x_2,\hat{x}_2)$ and for any $u(t)$:

$$\|f(x_1,x_2,u) - f(x_1,\hat{x}_2,u) + \xi(x_1,x_2,u)\| \le f^+. \quad (8)$$

Remark 2: The model (7), widely used as the dynamic equation for most mechanical systems and robotic manipulators [5,8], has a the relative degree of two from the control $u(t)$ to the output $y(t)$, which makes the design of a first-order SMO infeasible.

Using the super-twisting algorithm, a second order sliding mode observer for system (7) can be constructed as follows [10]:

$$\begin{aligned} \dot{\hat{x}}_1 &= \hat{x}_2 + z_1 \\ \dot{\hat{x}}_2 &= f(x_1,\hat{x}_2,u) + z_2, \end{aligned} \quad (9)$$

where the correction variables (z_1,z_2) are output injections of the form:

$$\begin{aligned} z_1 &= \lambda \|x_1 - \hat{x}_1\|^{1/2} sign(x_1 - \hat{x}_1) \\ z_2 &= \alpha sign(x_1 - \hat{x}_1). \end{aligned} \quad (10)$$

By denoting estimation errors $e_1 = x_1 - \hat{x}_1$ and $e_2 = x_2 - \hat{x}_2$, and taking into account condition (8), one can obtain the following differential inclusion:

$$\begin{aligned} \dot{e}_1 &= e_2 - \lambda \|e_1\|^{1/2} sign(e_1) \\ \dot{e}_2 &\in [-f^+, f^+] - \alpha sign(e_1), \end{aligned} \quad (11)$$

which is understood in the Filippov sense [19], i.e. the right hand is enlarged in some points to satisfy the upper semi-continuity requirement.

It was proven in [10] that, if design parameters α and λ are selected to satisfy the following condition:

$$\alpha > f^+$$
$$\lambda > q\frac{(\alpha + f^+)\sqrt{2}}{\sqrt{\alpha - f^+}}, \quad q > 1 \tag{12}$$

then the observer states $(\hat{x}_1, \hat{x}_2)$ in (9) will converge to (x_1, x_2) in finite time.

3. Illustrative examples

In the following, performance of first- and second-order SMOs will be evaluated for two nonlinear systems under linearization state feedback (SFB) and also output feedback control (OFB).

3.1 Example 1:

Consider the first and the second order sliding mode observers for following nonlinear system:

$$\dot{x}_1 = x_2$$
$$\dot{x}_2 = x_2{}^3 + u \tag{13}$$
$$y = x_1 .$$

To avoid the nonlinearity, feedback linearisation is used to place the closed-loop poles at $(-1 \pm j\sqrt{3})/2$. The state feedback controller for this system is constructed as follows:

$$u = -x_2{}^3 - x_1 - x_2 . \tag{14}$$

The output feedback controller is designed as:

$$u = -\hat{x}_2{}^3 - y - \hat{x}_2 . \tag{15}$$

The first-order sliding mode observer can be constructed as:

$$\dot{\hat{x}}_1 = \hat{x}_2 + L_1(y - \hat{x}_1) + K_1 sign(y - \hat{x}_1), \tag{16a}$$
$$\dot{\hat{x}}_2 = -y - \hat{x}_2 + L_2(y - \hat{x}_1) + K_2 sign(y - \hat{x}_1), \tag{16b}$$

where the observer gains $L = [L_1 \quad L_2]$ are chosen according to the desired eigenvalues of $s^2 + L_1 s + L_2 = 0$, and $K = P^{-1}C^T = [K_1 \quad K_2]^T$, with positive definite matrix P solving for the following Lyapunov equation:

$$(A - LC)^T P + P(A - LC) = -I ,$$

in which $A = \begin{bmatrix} 0 & 1 \\ 0 & 0 \end{bmatrix}$ and $C = [1 \quad 0]$.

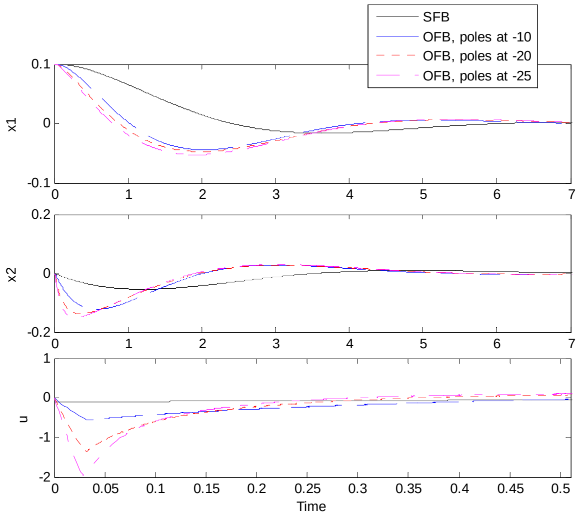

Fig. 1: State feedback and output feedback responses with different pole locations of a first-order SMO.

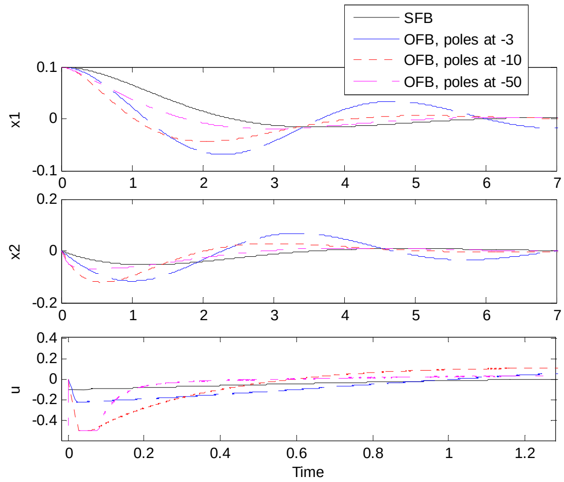

Fig. 2: First-order SMO responses with saturated output feedback

Figure 1 shows the output responses of the first-order SMO under output feedback and linearization state feedback, respectively. As the poles decrease, the error increases. Large negative poles often lead to faster estimation. It can also be seen that the control action u is greatly increased in magnitude with large negative poles. When the observer has a pole located at -250, a finite escape time of around 0.073 second due to the peaking phenomenon [20] can be observed.

With saturated output feedback, $|u| \le 0.5$, the peaking effect can be improved, as shown in Fig. 2. The time responses under output feedback in this case also approach the responses under state feedback when observer poles move towards the negative direction along the real axis. Even with poles larger than -250, the observer-based responses still show a convergence.

Let us now consider the proposed super twisting second-order SMO with the same control as in (15):

$$\dot{\hat{x}}_1 = \hat{x}_2 + \lambda \left| y - \hat{x}_1 \right|^{\frac{1}{2}} sign(y - \hat{x}_1), \tag{17a}$$

$$\dot{\hat{x}}_2 = -y - \hat{x}_2 + \alpha \, sign(y - \hat{x}_1), \tag{17b}$$

With feedback linearisation law (14), condition (12) will be less conservative for the selection of λ, α. Here, these parameters play the role of the variable structure control K_1, K_2 in the first order SMO (16). Figure 3 shows the control responses under non-saturated output feedback. They are faster but tend to exhibit the peaking phenomenon as the values of λ and α increase. A finite time escape will occur when the pole location is at around -150. This effect is reduced when using output feedback with saturated control ($|u| \le 0.5$), as shown in Fig. 4.

For performance comparison, responses using observer-based output feedback (OFB) are shown in Fig. 5 with conventional SMO and higher-order sliding mode observer (HOSMO) where saturation is imposed on the control signal. With observer poles located at -10, it is noticeable that the control action u in the case of twisting HOSMO is higher in magnitude than the in the case of SMO but the responses are much faster, resulting in more accurately following the SFB responses. As shown in Fig. 5, the peaking phenomenon has been limited by the saturation of the control signal.

To further evaluate the performance of HOSMO versus SMO, a step response of 0.1 for the first state is considered in an open loop test. The responses shown in Fig. 6 indicate that HOSMO is not only faster but also more accurate lower estimation error than SMO. Moreover, as depicted in the zooming-in figure, it is observed that there is no chattering for the HOSMO response while chattering does affects the state response in the case of SMO.

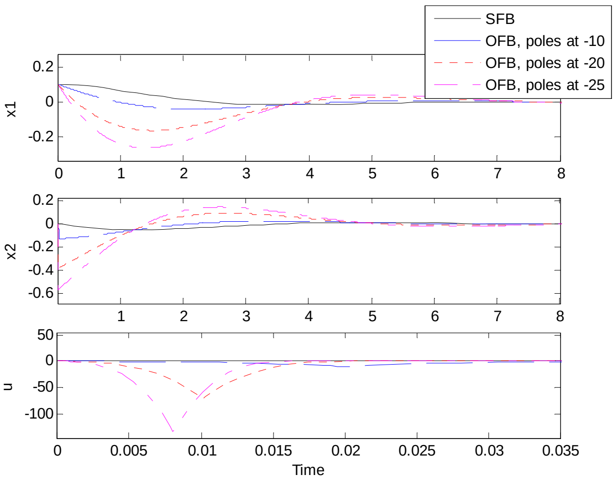

Fig. 3: State feedback and output feedback responses with different pole locations for second-order SMO.

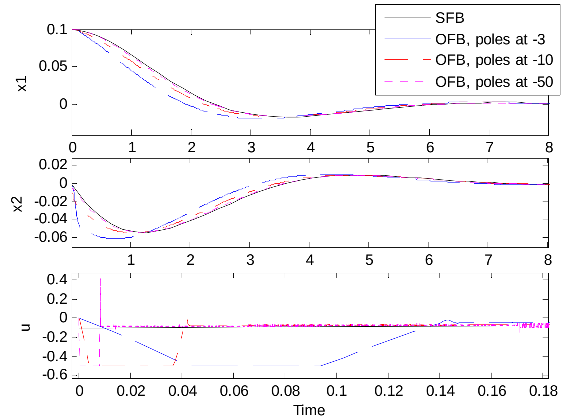

Fig. 4: State feedback and saturated output feedback with different poles for second order SMO.

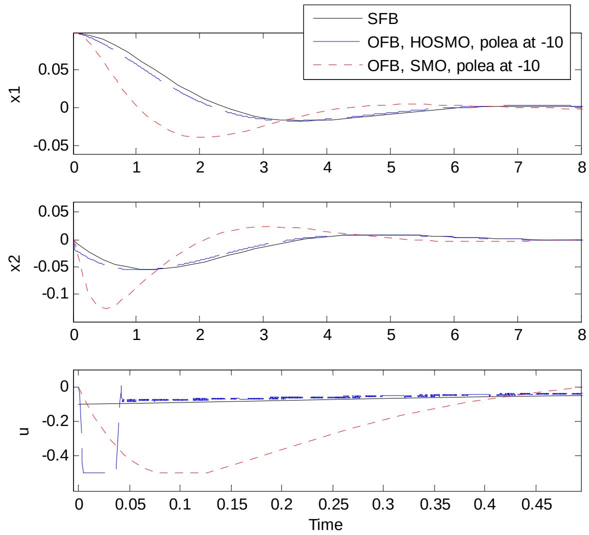

Fig. 5: Responses of saturated output feedback controller based on HOSMO and SMO with poles at -10.

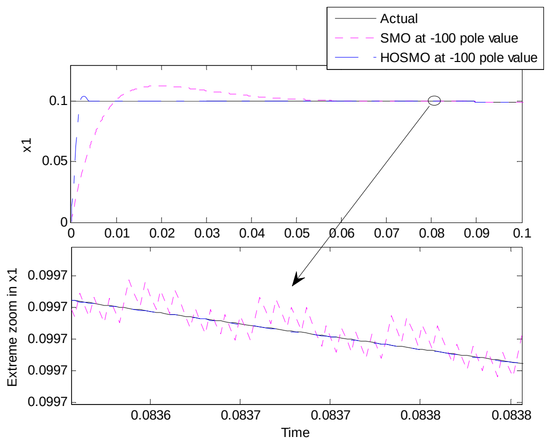

Fig. 6: Chattering effect of HOSMO and SMO with poles taken at -100.

3.2 Example 2:

Let us now consider a pendulum system described by:

$$ml^2\ddot{\theta} + mg_0 l\sin\theta + k_0 l^2\dot{\theta} = u(t). \qquad (18)$$

The state space equation is:

$$\dot{\theta} = \omega \qquad (19a)$$
$$\dot{\omega} = \frac{u}{ml^2} - \frac{g_0}{l}\sin\theta - \frac{k_0}{m}\dot{\theta}, \qquad (19b)$$

where the measurable output is angle θ.

If the continuous sliding mode state feedback (SFB) controller is designed [20]:

$$u = \frac{1}{c}[a\sin\theta + (b-\mu)\omega] - k\ sat\left(\frac{\omega+\mu\theta}{\varepsilon}\right), \qquad (20a)$$

then, the observer-based output feedback control is given by:

$$u = \frac{1}{\hat{c}}[\hat{a}\sin\theta + (\hat{b}-\mu)\hat{\omega}] - k\ sat\left(\frac{\hat{\omega}+\mu\theta}{\varepsilon}\right), \qquad (20b)$$

where $a = g_0/l$, $b = k_0/m$, and $c = 1/ml^2$ are the system constants depending on its parameters (mass *m*, damping k_0, length *l*, gravitational acceleration g_0), *k* is the variable structure control gain with boundary layer ε, and μ>0 is the slope of the sliding surface $\omega + \mu\theta$=0.

The sliding mode observer (SMO) in (3) can be constructed as:

$$\dot{\hat{\theta}} = \hat{\omega} + L_1(\theta-\hat{\theta}) + K_1 sign(\theta-\hat{\theta})$$
$$\dot{\hat{\omega}} = \underbrace{(\hat{c}u - \hat{a}\sin\theta - \hat{b}\hat{\omega})}_{\text{Nominal Plant}} + L_2(\theta-\hat{\theta}) + K_2 sign(\theta-\hat{\theta}), \qquad (21)$$

where the observer gains $L = [L_1 \quad L_2]$ are chosen according to the desired eigenvalues of $s^2 + (L_1+\mu)s + L_2 = 0$, and $K = P^{-1}C^T = [K_1 \quad K_2]^T$, with positive definite matrix *P* solving for LMI (6) in which $A = \begin{bmatrix} 0 & 1 \\ 0 & -\mu \end{bmatrix}$, $C = [1 \quad 0]$, and Lipschitz constant $\gamma = a$.

In the simulation, the actual plant parameters were taken as $a = 9.3429$, $c = 6.0469$, *b*=1, with their nominal estimates $\hat{a} = 9.81$, $\hat{c} = 10$, $\hat{b} = \mu = 1$. We also considered the third case, when $\hat{a} = \hat{c} = 0$ in (21), i.e. (a linear high-gain observer). The SFB responses are used as a benchmark for all cases.

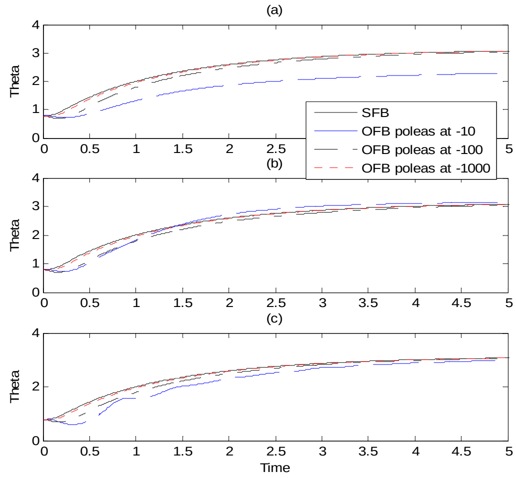

Fig. 7: SMO position estimates with (a) nominal parameters, (b) actual plant, and (c) linear high gain observer.

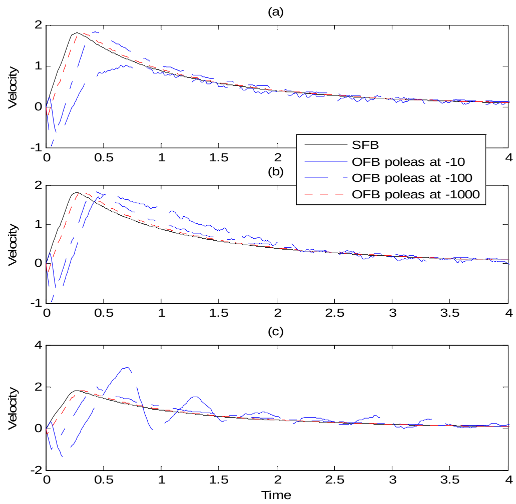

Fig. 8: SMO velocity estimates with (a) nominal parameters, (b) actual plant, and (c) linear high gain observer.

As shown in Figs. 7 and 8 respectively for estimates of the angle θ and angular velocity ω, the output feedback responses tend to approach the state feedback responses at higher observer poles. In the figures, we used three different sets for observer (21) with actual plant parameters (a), nominal plant parameters (b), and linear high gain observer (c). When poles are relatively large, the nominal plant apparently does not affect much on the improvement of the estimation performance. This is expected because increasing the values of poles will yield higher robustness with against the system uncertainty.

From (9-10), the super-twisting higher-order sliding mode observer (HOSMO) for system (19) is:

$$\dot{\hat{\theta}} = \hat{\omega} + \lambda\left|\theta-\hat{\theta}\right|^{\frac{1}{2}} sign(\theta-\hat{\theta})$$
$$\dot{\hat{\omega}} = \left(\hat{c}u - \hat{a}\sin\theta - \hat{b}\hat{\omega}\right) + \alpha\ sign(\theta-\hat{\theta}), \qquad (22)$$

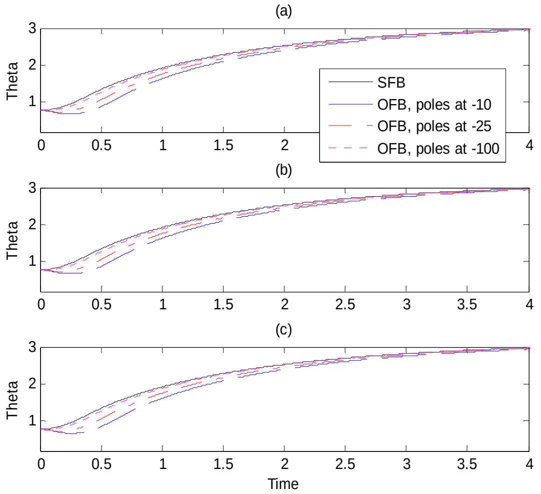

Fig. 9: HOSMO position estimates with (a) nominal parameters, (b) actual plant, and (c) linear high gain observer.

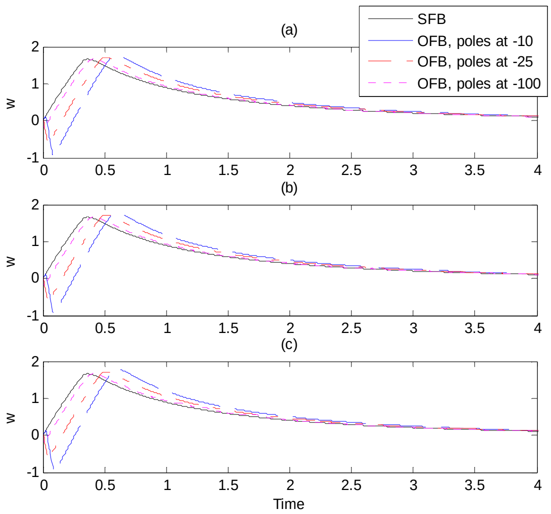

Fig. 10: HOSMO velocity estimates with (a) nominal parameters, (b) actual plant, and (c) linear high gain observer.

where parameters λ, α are chosen according to (12). Figures 9 and 10 show the estimates of the first and second states, namely the pendulum's position and angular speed, respectively. We can see in all cases (a), (b) and (c) that the output feedback responses approach the state feedback responses in finite time. It can be expected that robustness of the estimation against uncertainty on the nominal plant is improved as the poles increase. By using larger poles (-100), OFB responses are almost coincident with SFB responses in face of a wide range of system's parametric variations.

Notably, a close comparison between SMO and HOSMO responses, shown respectively in Figs 7,8 and Figs. 9,10, also indicates the outperformance of the higher-order sliding mode observer over the conventional one in terms of estimation accuracy.

4. Conclusion

This paper has presented a refinement of the design of first-order and higher-order sliding mode observers for nonlinear systems. A comparison study is given to illustrate the estimation performance of these observers for two nonlinear systems using state feedback and observer-based output feedback control. Some advantages of the super-twisting second-order sliding mode observers over the conventional ones are shown in the simulation results.

Acknowledgments

This work is supported, in part, by the Centre of Excellence programme, funded by the Australian Research Council (ARC) and the New South Wales State Government. The second and fourth authors would like to gratefully acknowledge UTS research grant 2006000848.

References

[1] D. Luenberger, "Observers for multi variable systems", *IEEE Trans. Autom. Control*, Vol. 11, pp. 190-197, 1966.

[2] V. Utkin, "Variable structure systems with Sliding Modes", *IEEE Trans. Autom. Control*, Vol. 22, pp. 212-222.

[3] S. Spurgeon, "Sliding Mode Observers: a Survey," *Int. J. Systems Science*, Vol. 39, No. 8, pp. 751-764, 2008.

[4] J.J.E. Slotine, J.K. Hedrick, and E.A. Misawa, "On sliding observers for nonlinear systems," *Proc. of the American Control Conference*, pp. 1794-1800, Seattle, USA, 1986.

[5] M. Saif, W. Chen, and Q. Wu, "Higher order sliding mode observers and differentiators- application to fault diagnosis problem," in *Modern Sliding Mode Control Theory*, Bartolini *et al.* (Eds.), LNCIS Springer-Verlag, Berlin 2008, pp. 321-324.

[6] Q.P. Ha, A. Bonchis, D.C. Rye, and H.F. Durrant-Whyte, "Variable structure systems approach to friction estimation and compensation", *Proc. of the Int. Conference on Robotics and Automation*, California, USA, pp. 3543-3548, 2000.

[7] A. Levant, "Higher-order sliding modes, differentiation and output-feedback control," *Int. J. Control*, Vol. 76, No. 8, pp. 924-941, 2003.

[8] G. Bartolini, A. Pisano, E. Punta, and E. Usai, "A survey of applications of second-order sliding mode control to mechanical systems," *Int. J. Control*, Vol. 76, No. 9/10, pp. 875-892, 2003.

[9] H. Dalvand, H.T. Nguyen, and Q.P. Ha, "Design of second-order sliding mode controllers for MR damper-

embedded smart structures," *Proc. Int. Symp. Automation and Robotics in Construction*, Austin, Texas, US, pp. 332-340, 2009.

[10] J. Davila, L. Fridman, and A. Levant, "Second Order Sliding Mode Observer for Mechanical Systems", *IEEE Trans. Automatic Control*, Vol. 50, No. 11, pp. 1785-1789, 2005.

[11] V. Lebastard, Y. Aoustin, F. Plestan, and L. Fridman "Absolute Orientation Estimation Based on Higher Order Sliding Mode Observer for Five Link Walking Biped Robot", *Proc. International Workshop on Variables Structure Systems*, Alghero Italy, pp. 373-378 June 2006.

[12] A. Rabhi, N.K. M'sidiri, L. Fridman, and Y. Delanne "Second Order Sliding Mode Observer for Estimation of Road Profile", *Proc. International Workshop on Variables Structure Systems*, Alghero Italy, pp. 161-165, June 2006.

[13] H. Sharim, M. Ouladsine, and L. Fridman, "Vehicle parameter and state estimation via sliding mode observers", in *Modern Sliding Mode Control Theory*, Bartolini *et al*. (Eds.), LNCIS Springer-Verlag, Berlin 2008, pp. 345-362.

[14] Y. Huangfu, W. Liu, and R. Ma, "Permanent magnet synchronous motor fault detection and isolation using second order sliding mode observer," *Proc. 3rd IEEE Conference on Industrial Electronics and Applications*, Singapore, pp. 639-644, 2008.

[15] H. Saadaoui, M. Djemai, N. Manamanni, T. Floquet, and J.P. Barbot, "Exact Differentiation via Sliding Mode Observer for Switched Systems", *Proc. 2nd IFAC Conference on Analysis and Design of Hybrid Systems*, Alghero, Italy, pp. 124-129, June 2006.

[16] Q.P. Ha and H. Trinh, "Simultaneous state and input estimation for a class of nonlinear systems", *Automatica,* Vol. 40, pp. 1779-1785, 2004.

[17] W. Wang and Z. Gao, "A comparison study of advanced states observer design techniques", *Proceedings of the American Control Conference*, Denver, Colorado, pp. 5774-4759, 2003.

[18] A. Alessandri, "Sliding-mode estimators for a class of nonlinear systems affected by bounded disturbances," *Int. J. Control*, Vol. 76, No. 3, 2003, pp. 226-236.

[19] A.F. Fillippov, *Differential Equations with Discontinuous Right-Hand Sides*, Dordrecht, The Netherlands: Kluwer, 1988.

[20] H.K. Khalil, *Nonlinear Systems*, 3d Edition, Prentice-Hall, New Jersey, 2002.